

Performance Enhancement of Multi-Area Interconnected Power System using Revolutionary Energy Balance Control

B. Prakash Ayyappan*, R. Kanimozhi**

*V.S.B Engineering College, Karur, Tamilnadu, India. 639 111 (e-mail: prakashayyappan78@gmail.com)

**University College of Engineering, Anna University-BIT Campus, Tiruchirappalli, Tamilnadu, India.620 024 (e-mail: kanimozhi_17@aubit.edu.in)

Abstract: In the current situation of the power system, with the need to increase power to meet the availability of all types of loads, the quality of power is equal to the demand. On this day, there is no change, and a demanding power supply with a stable and reliable power supply at all times. Therefore, in order to maintain the quality and power to meet the current reforms in the energy sector and to adapt to the changes in the demands of the industrial sector thus changing in frequency, an advanced controller is necessary. This work presents a Revolutionary Energy Balance Control (REBC) controller approach for Automatic Generation Controller (AGC). This AGC method focuses on balancing the whole generating system while maintaining a consistent system frequency per tie-line power flow, with no load changes or power losses. In a Multi-Area Interconnected Power System (MIPS), a sudden load fluctuation, on the other hand, causes non-linearity (frequency deviation and tie-line) in all control regions. To lower the maximum deviation and oscillation duration, modelling error is taken into consideration. The main objective of FP-PID-based AGC is to preserve power system stability and reliability. The proposed technique is compared to standard two-area and three-area systems using data acquired in Simulink/MATLAB. The results show that the proposed technique has high dynamic responsiveness, economical operation, low magnitude error, and low frequency transients in MIPS. The performance of the REBC controller will be evaluated and compared with existing control technique using metrics such as settling time, steady-state error, THD, and efficiency.

Keywords: Multi-Area Interconnected Power System, frequency control, Revolutionary Energy Balance Control, Resilience Random Variance Reduction Technique.

1. INTRODUCTION

In order to run a reliable and stable electrical power system, a system frequency should be kept at a specified value or its deviation should be adjusted as quickly as possible in the event of load supply or demand changes. In a steady-state condition, a power system's whole capacity is used to supply loads. A sudden and abrupt shift in the load demand causes a mismatch between the load and the generated power. The MIPS power demand varies as a result of this circumstance. As a result, a control system is required to eliminate the mismatch problem by lowering the frequency and amount of tie-line power failures (Prakash Ayyappan et al., 2021; Anbarasi et al., 2016). To address these issues, this system proposed a sophisticated controller that combines a traditional PID controller with an adaptive controller known as the REBC controller. These methods are simple to use, provide quicker convergence, and only require a few parameters to correctly set up AGC development (Dong et al., 2017; Lackner et al., 2020). This work employs the suggested REBC controller to provide good frequency regulation, estimate weighted load power, and investigate the nonlinear feature in error signals in multi-area, multi-source (thermal, PV, wind, and hydro) controlled power systems. A considerable Frequency Deviation (FD) is maintained under control because the REBC controller controls the flow of power in the tie-line from one location to another. A power analysis between unregulated load and power load violation is done to demonstrate the best of the proposed controller (Xu et al., 2016; Daraz et al., 2020; Li et

al., 2016). The suggested approach has been proved to be better in terms of settling time (sec), steady-state error (%), THD (%), and efficiency (%). Finally, compare the performance of the proposed technique to that of existing state-of-the-art approaches. For the improvements of Multi-Source and Multi-Area system for stability in the proposed system, it needs to identify the drawback in the conventional methods that are given below. The Load Frequency Control is a fundamental mechanism in the interconnected power system. To deliver high-quality, reliable, and stable electrical power, the designed controller must function efficiently, that is, it must suppress regional frequency and tie-line power deviations (Vijayakumar et al., 2016; Fakharian et al., 2016; Pathak et al., 2018). In this work, the LFC issue in multi-area power systems is solved using the Higher-Order Differential Feedback Controller (HODFC) and a created Fractional Order Differential Feedback Controller (FHODFC) (Daraz et al., 2020; Van Van Huynh et al., 2018). A Virtual Generation Ecosystem Control (VGEC) approach that uses the time tunnel concept and the concept of new criteria to accomplish rapid automatic generation control power dispatch and optimum micro grid coordination (Apostolopoulou et al., 2016; Beyda et al., 2015; Chen et al., 2019). This system presents the first theoretical stability analysis of AGC in a nonlinear power system that is interconnected. This Analysis is focused on singular perturbation theory, and it provides theoretical support for the widely held idea that AGC aids in the stabilization of systems operating on normal timescales (Zhang et al., 2018; Xi et al., 2020). The Area Control Error

(ACE), also known as the Area Injection Error (AIE), involves direct monitoring of generator power levels in the condition of bias uncertainty and nonlinearity in generator turbine-governor reactions, this results in improved AGC performance (Simpson-Porco et al., 2021; Ganger et al., 2018; Kammer et al., 2019; Li et al., 2020; Liu et al., 2015). A Dynamic Regulation Market Mechanism (DRMM) is presented in this system, which allows Demand Response (DR) units and generators to compete for regulation service in real time, assuring optimal allocation and lowering regulation service costs (Patel et al., 2019; Prostejovsky et al., 2018). When variable wind power is incorporated into power systems, the desired response may not be obtained. This work presented a Dynamic Gain Tuning Control (DGTC) technique for AGC to overcome these PQ issues (Sahin et al., 2020; Tan et al., 2020). This methodology is for evaluating the influence of various types of faults in the measurements used by the AGC system on power system dynamic performance. The statistics of system state variables are evaluated using stochastic system analysis approaches to address the random character of these errors. The convergence properties of these statistics are used to discover errors that cause instability (Shiltz et al., 2019; Qiu et al., 2020). Multi-area AGC's primary responsibilities include coordinating power exchange throughout subareas as well as maintaining power balance. By accomplishing cooperation among the participating generators, which are situated in different subarea networks that are interconnected, the newly established new power flow model enables multi-area AGC. (Wang et al., 2019; Zhang et al., 2018).

2. MULTI SOURCE INTERCONNECTED SYSTEM

The objectives of this work is to employ AGC to keep a nominal frequency deviation and tie-line power flow for Multi source interconnected power system. Maintaining a constant frequency with the speed governor is challenging for the MIPS system in coastal areas where the power supply is obtained from these sources like solar, wind, thermal and hydro power stations, thus it must be controlled to provide high-quality power in tie-line. As a result, a unique control mechanism has been developed to balance the effect of dynamic load fluctuations while maintaining a nominal frequency. Overall, the controller structure and accurate controller REBC control algorithm are obviously dependent on the optimal performance of the Power Supply System to decrease power loss and Frequency variation in the MIPS. In multi-area AGC, the REBC controller is used. There are four types of power plants in each area: thermal, wind, solar, and hydroelectric. This controller ensures that the power system runs smoothly and consistently. The suggested technique's performance is compared to that of many types of current controllers in two and three locations. The proposed technique is competitively superior, resilient, and stable in the event of a change in system features and random load disturbance. Based on this analysis, the proposed approach reduces the ACE errors' settling time per frequency and the oscillation of the current flow on the tie-line at each location. As a result, the suggested AGC controller might be used in real-time power supply system operation.

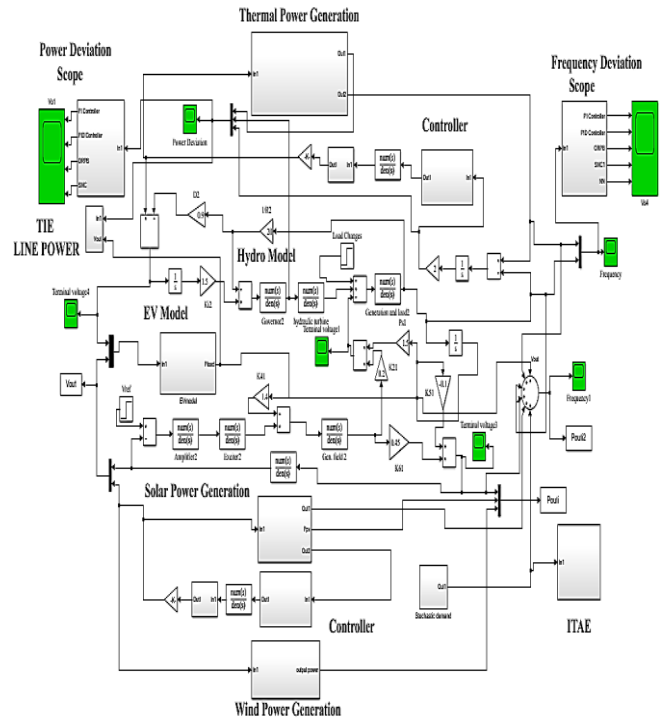


Fig. 1. Power system model of three-area with multi-source.

2.1 Solar power generation

To generate the appropriate Voltage (V) and current (I), using a solar power system consists of many series and parallel coupled solar cell. The connection between V and I is non-linear due to that Solar radiation and load current influence the maximum power output of a PV array. As a result, a control strategy is necessary to obtain the greatest power from solar radiation. A PV system's output power may be stated as;

$$P_{EPV} = \eta S \phi [1 - 0.005 (T_a + 30)] \quad (1)$$

Where T_a represents the ambient temperature ($^{\circ}\text{C}$), S represents the PV array's measured area (m^2), ϕ represents solar irradiation (kW/m^2), and η represents the PV array's conversion efficiency (%). The transfer function of a solar system may be calculated using a simple linear first-order lag equation (4).

$$G_{PV}(S) = \frac{\Delta P_{PV}}{\Delta \phi} = \frac{K_{PV}}{1 + sT_{PV}} \quad (2)$$

Where K_{PV} is gain constant and T_{PV} is a time constant.

2.2 Wind Generator (WG)

The air density and wind speed control the amount of electricity generated by wind power facilities. Where equation (3) shows how these two parameters influence the amount of power generated.

$$P_{WIND} = \frac{1}{2} \cdot ab \cdot \rho \cdot B_i \cdot V^3 \quad (3)$$

Where αb =Sweep area of blade in m^2 , ρ = air density, βi = power co-efficient of air.

The following is an example of the WG transfer function model:

$$G_{WIND}(S) = \frac{\Delta P_{Wind}}{P_{Win}} = \frac{K_{WTG}}{1 + s.T_{WTG}} \tag{4}$$

K_{WTG} =wind turbine gain,

T_{WTG} =Time based turbine gain

2.3 Thermal Generator

The thermal generator model in the LFC research has four components. The transfer functions of governors, steam turbines, governors, and re-heaters are among these components. Figure 2 illustrates the heat generator's transfer function model, which includes all components.

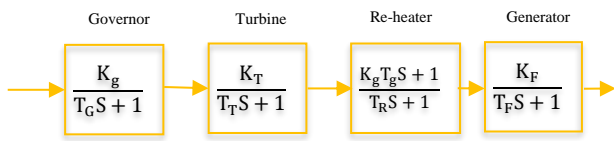


Fig. 2. Transfer function model of the thermal generator.

The Frequency regulation is improved by two control loops in the heat-generating structure. The heat-generating unit assists in the frequency adjustment of the governor from the first cycle. Even if the first cycle is useful for detecting large frequency fluctuations, the constant-level inaccuracy in the frequency signal is a major concern in the implementation of this control loop. As a result, Area Control Error (ACE) supplemental loop signals can be used to reduce static error. The ACE signal is expressed mathematically as follows:

$$ACE_i = \Delta P_{tie,i} + \beta_i \Delta f_i \tag{5}$$

The regional bias factors of the network connection, tie-line power, and FD of the i-th area, respectively, are $\beta_i, \Delta P_{tie,i}$ and Δf_i in this study. The heat generator's basic construction contains two frequency control loops, which will be discussed in the next section.

2.4 Hydropower generation

The main mover slows to compensate for the power imbalance, but the power generation controls the speed. As the speed change decreases, the error signal lowers, and the governor speed becomes constant. Because the load changes over time, it is difficult to set the governor speed to a fixed value; hence, this system employs a control system with an integrator. To eliminate offsets, the control system analyses the change and adapts as needed. A system's reset point refers to its capacity to return to its starting state. As a result, the AGC is a frequency-adjustment mechanism that does so automatically. The AGC for a given site is depicted in Figure 3. The AGC is made up of a governor device that sends a

signal to the turbine to change its speed in order to maintain a consistent frequency.

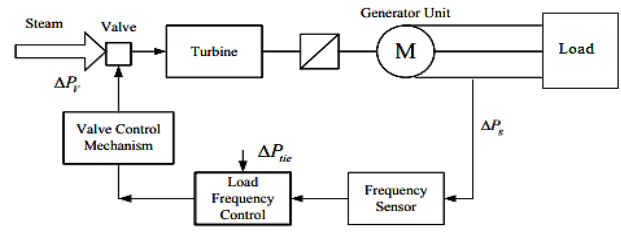


Fig. 3. Functional block for the thermal generator.

The system's three most important components are the governor, prime mover load, and inertia model. The system's block diagram, represented in Figure 4, may be expressed using equations (6 to 8). The following is a list of them:

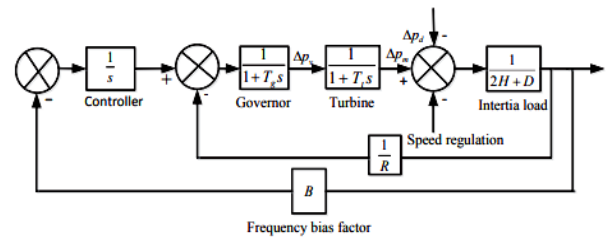


Fig. 4. Control block diagram for the thermal generation.

Governor model

The hydraulic amplifier converts the command ΔP_g to the position of the steam valve ΔP_v . T_g is the governor's time constant, and the equation 6 is the governor's transfer function.

$$\frac{\Delta P_{v(s)}}{\Delta P_{g(s)}} = \frac{1}{1 + T_g s} \tag{6}$$

2.4.1 Prime mover model: The speed load characteristic equation may be used to examine the motor load, which is sensitive to frequency changes. As indicated in equation (7), the prime mover model, ΔP_m couples the mechanical power output to the change in the ΔP_v steam valve.

$$\frac{\Delta P_{m(s)}}{\Delta P_{v(s)}} = \frac{1}{1 + T_t s} \tag{7}$$

2.4.2 Load and inertia model: The speed load characteristic equation may be used to examine the motor load, which is sensitive to frequency changes. (8).

$$\frac{\Delta P_{m(s)}}{\Delta P_m - \Delta P_I} = \frac{1}{2H + D} \tag{8}$$

Frequency bias factor: As mentioned in equation, (9) the frequency biased factor is the sum of frequency-sensitive load change (D) and speed regulation (9).

$$B = \frac{1}{R} + D \tag{9}$$

2.5 Design of Revolutionary Energy Balance Control Algorithm controllers

In this work, a novel Revolutionary Energy Balance Control Algorithm (REBC) controller is implemented as a FOPID controller to change the parameters like voltage, current and frequency of a multi-area power system. In comparison to conventional controllers, fractional-order controllers offer additional tuning options, higher responsiveness with high order, and non-minimum phase systems. The integral portion, on the other hand, enhances the steady-state response in a normal Proportional Integral Derivative (PID) controller. On the other aspect, it causes system response to be delayed and diminishes relative stability. The derivative element enhances dynamic responsiveness, speeds up the system, and increases stability. Furthermore, it increases the system's sensitivity to noise disruptions. In this system utilize a fractional-order controller to balance the advantages and disadvantages of a standard PID controller. In this work the fractional integral/derivative portion was used instead of the pure integral ($\frac{1}{s}$) derivative (s) part. The proposed FOPID-based REBC controller is represented in Figure 5 as a block diagram. The FOPID-based REBC controller's input signal is f , and its output "y" is transmitted to the next stage controller, the (1+PI) controller, to generate the presented FOPID-(1+PI) controller's final response, as shown in Figure 5. In addition to the FOPID control signals, the controller described here is also available (10, 11).

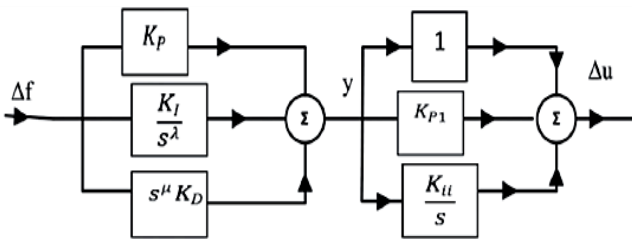


Fig. 5. Block diagram for the FOPID based REBC controller.

$$Y = K_p \Delta f + K_{I_s^{-\lambda}} \Delta F + K_p s^\mu \Delta f \tag{10}$$

$$\Delta u = [(K_p \Delta f + K_{I_s^{-\lambda}} \Delta F + K_p s^\mu \Delta f)] X [(1 + K_{p1} + K_{i_{s^{-1}}})] \tag{11}$$

In simulation or other practical applications, the integer order transfer function is necessary to generate fractional-order differentiators or integrators. Infinite-dimension fractional-order differentiators or integrators in the relevant frequency range must be approximated in order to do so. This is evaluated using time-domain rational approximation methods and sub-optimal approximation methodologies. The transfer function of a filter in the considered frequency range (ω_b, ω_h) is (12).

$$G_{rationalfilter(s)} = K \pi_K^N = -N \left(\frac{s + w_1}{s + w_1} \right) \tag{12}$$

The rational filter's zeros, poles, and gain are provided by (13), (14), and (15), respectively.

$$W_1' = W_b \left(\frac{W_h}{W_b} \right)^{\frac{1+N + \frac{(1-\beta)}{2}}{2N+1}} \tag{13}$$

$$W_1 = W_b \left(\frac{W_h}{W_b} \right)^{\frac{1+N + \frac{(1-\beta)}{2}}{2N+1}} \tag{14}$$

$$K = W \frac{\beta}{h} \tag{15}$$

The integrator/order differentiator's is "2N+1," whereas β the filter's order is "2N+1." For all fractional-order elements, the fifth-order time-domain approximation in the frequency region of 0.01, 100 radian per sec has been addressed. The Load Frequency (LF) is reduced by utilizing a low-order approximation, but the amplitude and phase responses of ripple production are increased.

2.6 Proposed system Revolutionary Energy Balance Control Algorithm

The determination of sudden and random variation has a direct effect on the system dynamics and is just as significant as the optimization approach's performance. Sudden and random variation should be used to achieve goals like rapid and non-oscillated system response with low overshoot and steady-state inaccuracy. The use of Revolutionary Energy Balance Control (REBC) in control engineering allows for more accurate system modelling or control system design, as well as greater robustness and adaptability. The finite tuning of Revolutionary Energy Balance Control (REBC) algorithm's steps by means of Fractional order controller are described below.

2.6.1 REBC Algorithm Steps

- Step 1: Initialization of devices.
- Step 2: Initially, the source power is turned on.
- Step 3: Define the objective function in which the design variables are constrained equally and unequally.
- Step 4: Set the population size to the iteration number, and the design variables to the DG and location sizes.
- Step 5: Determine the value of the goal function using the forward-backward load flow.

$$F(X) = \min \sum_{l=1}^b R_l * I_l^2 \tag{16}$$

Step 6: Set the number of iterations to 1 and look for the best population/learner with the best objective function value. Calculate the population's mean as well.

Step 7: Update the previous solutions with the following statement, then go on to all acceptable solutions that are better than current teacher's.

$$D_M_{s,k} = r_K (X_{s,kbest,k} - T_D M_{s,k}) \tag{17}$$

In the subject "s," is the best learner's (or teacher's) outcome TD is the Training Quality Factor, which is the root reason

for enhancing or modifying the mean class result in that subject $x_{s,kbest,k}$ is a uniformly distributed random integer between [0, 1], and TD is the Training Quality Factor, which is the root reason for enhancing or modifying the mean class result in that subject $M_{s,k}$. The Fractional Order Controller (FOC) can be either 1 or 2, and it is selected at random with equal probability as shown in Equation.

Step 8: Using the Equation below, modify the solutions obtained in step 5 and carry forward any acceptable options that result in a better solution than the current position.

$$X'_{i,s,k} = X_{i,s,k} + DM_{s,k} \tag{18}$$

All updated $X'_{i,s,k}$ values generate a better function value, they are used as input for the next cycle/iteration; otherwise, they are left unchanged.

Step 9: Repeat steps 6–8 until the total number of iterations reaches the maximum number of iterations.

Step 10: Finally, represent the best solution/teacher as the best solution, plot the best position records from all iterations as convergence characteristics, and then stop.

This best solution can be correspondingly gives the parameters voltage, current and frequency for achieving better performance results like steady state error, settling time, overshoot, integral time absolute error and also the efficiency of the system.

3. SIMULATION MODEL WITH RESULT AND DISCUSSION

The simulation diagram for the Multi-Source and Single-Area (MSSA) Interconnected Power System is shown in Figure 6.

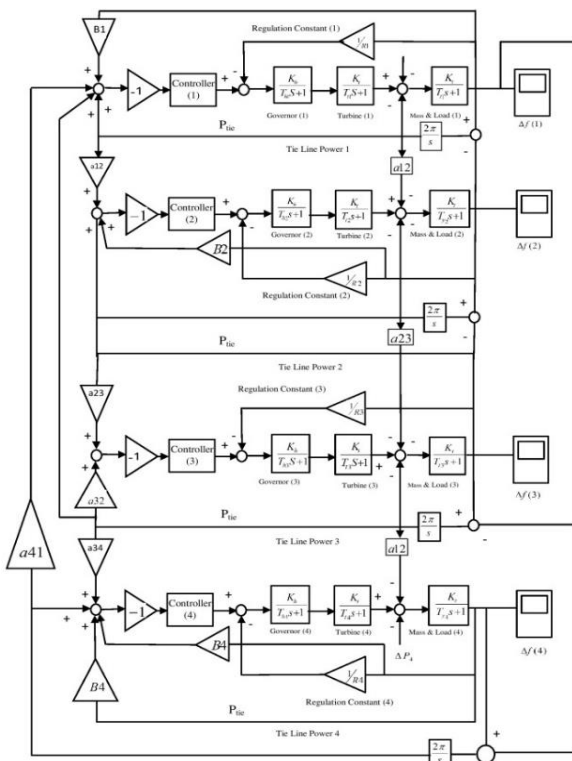


Fig. 6. Simulation Model for Multi-Source and Single Area Interconnected system.

The performance of interconnected power systems is evaluated under various load circumstances in this MSSA (20%, 50%, and 100 %). Performance measures such as steady-state error (%), settling time (sec), Overshoot (%), Integral Time Absolute Error (ITAE), and efficiency (%) are examined using various control methodologies based on the test data. The results of the various load condition-based tests are shown in the figures and tabulations below.

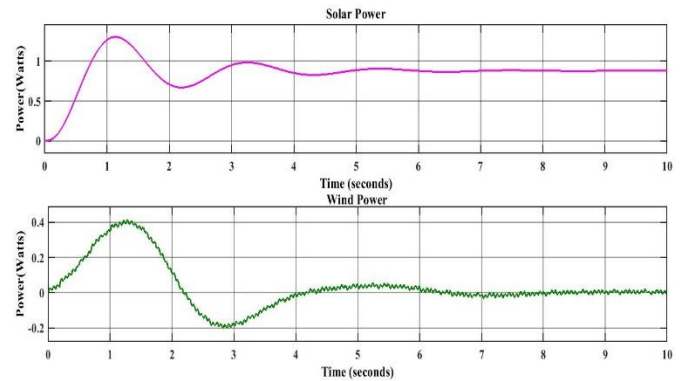


Fig. 7. Solar and wind generation waveform.

Figure 7 illustrates solar and wind energy generation; the above waveform depicts power generation throughout various periods. Feedback is delivered to the FOPID in order to sustain both the solar and wind generating singles fluctuations. An automated generation control is offered as a result of this procedure, and the generated power is regulated. The energy deviation of the solar and wind generation systems is analyzed based on the load system's operating state, as shown in the figures.

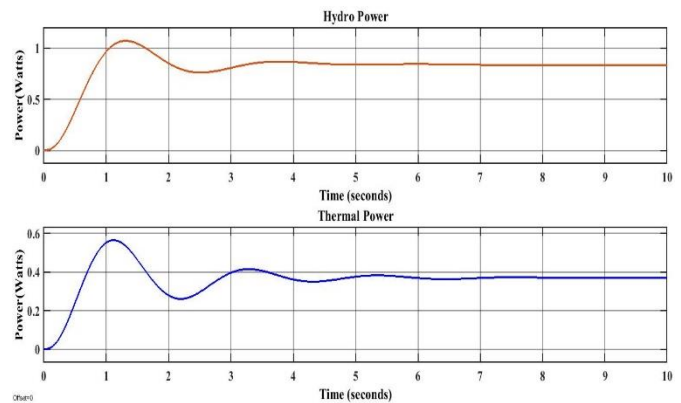


Fig. 8. Thermal-hydro Power Generation Waveform.

Figure 8 represents multi-power generating waveforms, also known as thermal and hydro power-producing. The power-producing facilities are used as auxiliary power sources in the Multi-Source and Single-Area (MSSA) Interconnected Power System, which successfully balances the grid power line under dynamic load fluctuation scenarios. The proposed REBC based converter system continually provides energy for the bus system due to the thermal and hydropower producing systems. As shown below, the performance of the MSSA connected power system was examined under various load circumstances, including 20%, 50%, and 100%.

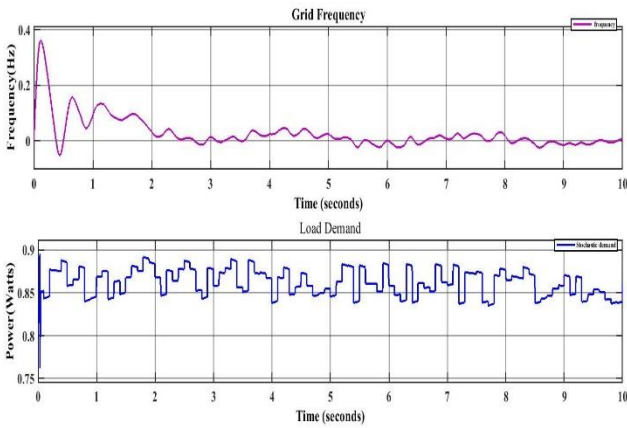


Fig. 9. Grid frequency with 20% load varying system.

Figure 9 shows the suggested grid frequency analysis, which is based on the REBC algorithm, and is tested with various stochastic load demands. The system's dynamic load fluctuation will create higher frequency variation, however, the suggested REBC would produce reduced frequency variation during 20 percent load circumstances.

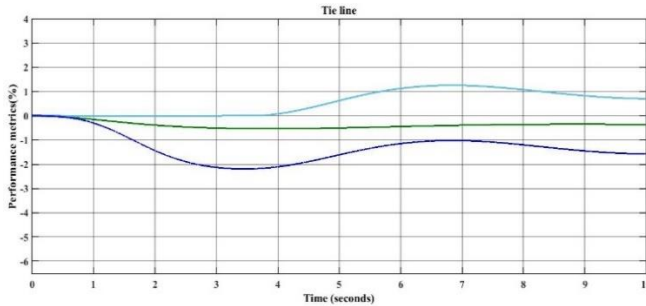


Fig. 10. Tie Line power stability analysis.

When comparing several controllers such as the PI, PID Figure 10 shows the tie-line power stability investigation of the recommended multi-source-single area interconnected model under dynamic load shifting, and REBC controllers, the REBC controller produces a better result.

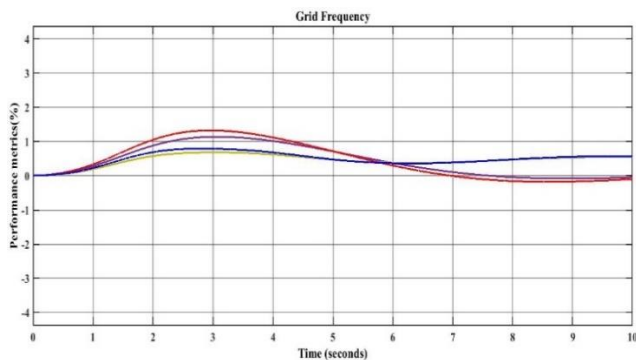


Fig. 11. Grid frequency based on different control approaches.

The grid frequency and outcome of Integral Time Absolute Error (ITAE) employing various control approaches is shown in Figure 11 and 12, in that Revolutionary Energy Balance Control calculates a 1.46% error ratio based on this ITAE analysis.

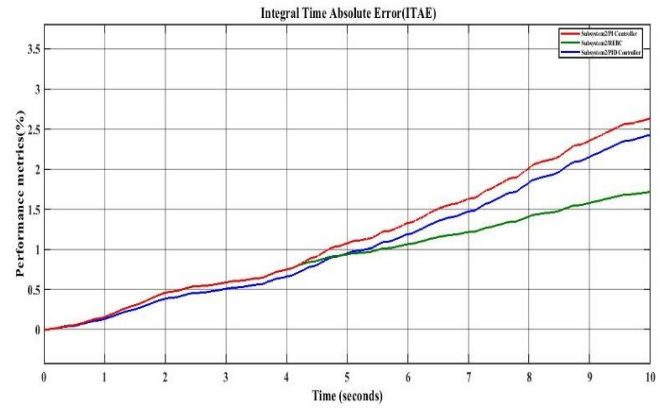


Fig. 12. ITAE using different control technique.

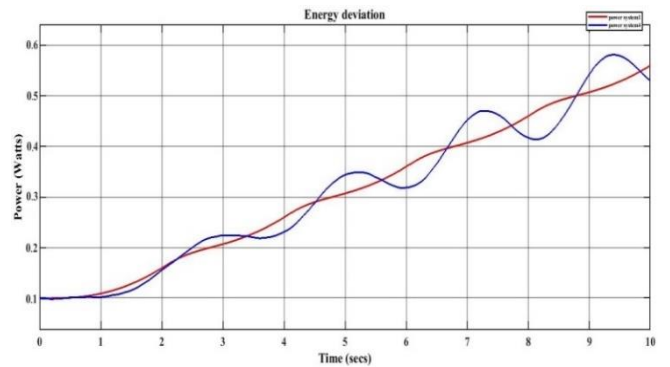


Fig. 13. Energy deviation using different control techniques.

The maximum amount of load change for the MSSA Interconnected Power System is shown in Figure 5.13. The suggested REBC controller performs better in both power system 1 (solar) and power system 2 (wind) energy sources under 20 percent load-changing situations.

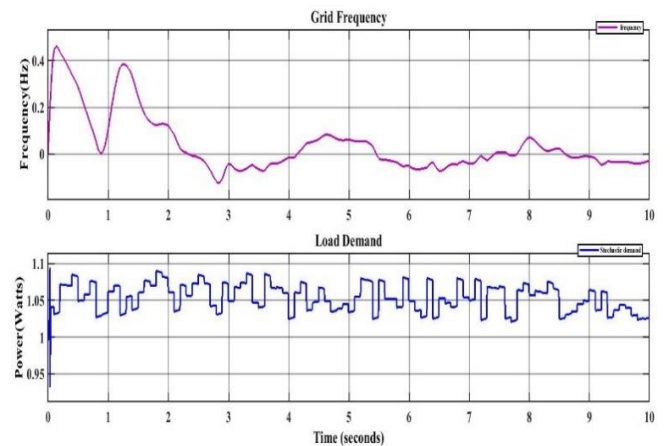


Fig. 14. Grid frequency with 50% load varying system.

Figure 14 illustrates the suggested grid frequency survey, which is based on the REBC algorithm and tested with various stochastic load demands.

The system's dynamic load shift will create higher frequency fluctuation, however, the suggested REBC would provide reduced frequency variation during 50 percent load circumstances, as illustrated in Figure 15.

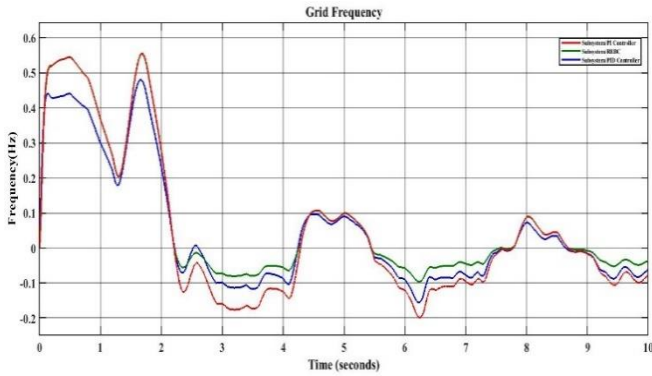


Fig. 15. Grid frequency based on different control approaches.

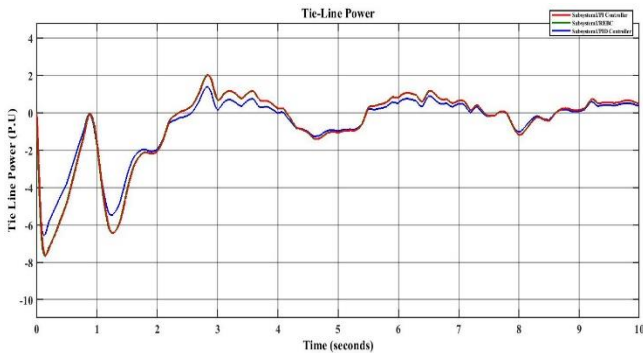


Fig. 16. Tie Line power stability analysis for 50% load system.

Figure 16 represents the suggested multi-source-single-area interconnected model's tie-line power stability study for 50 percent load changing circumstances. In a comparison of several controllers, the REBC controller outperforms the PI, PID, and REBC controllers under 50 percent load-changing situations.

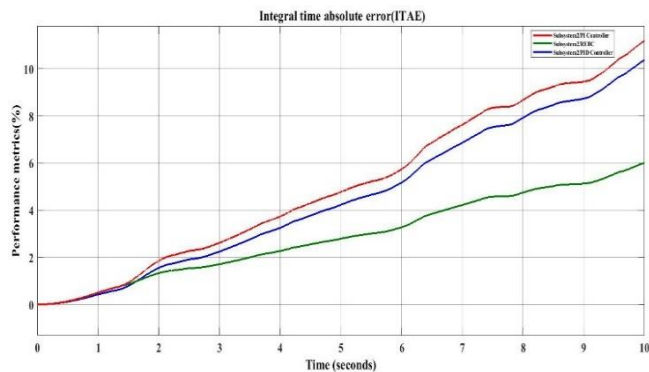


Fig. 17. ITAE using different control technique.

Figure 17 shows Integral Time Absolute Error (ITAE) using various control methodologies under 50 percent load fluctuation circumstances. Based on this ITAE analysis, REBC calculates a 2.0 percent error ratio.

The maximum amount of load change for the MSSA Interconnected Power System is shown in Figure 18. Variable conditions are studied for 50 percent load; the suggested REBC controller performs better in power system 1 (solar) and power system 2 (wind) energy sources.

Figure 19 demonstrates a suggested grid frequency survey based on the REBC algorithm, with several stochastic 100 percent load demand situations being examined.

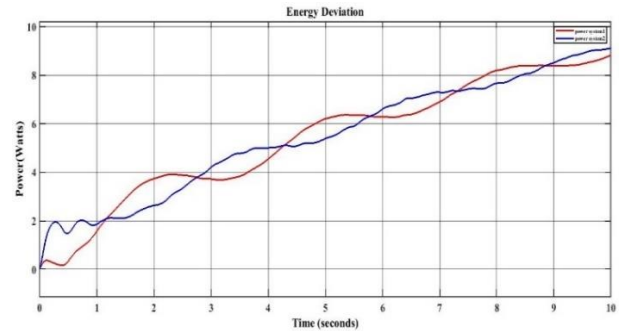


Fig. 18. Energy deviation using different control techniques.

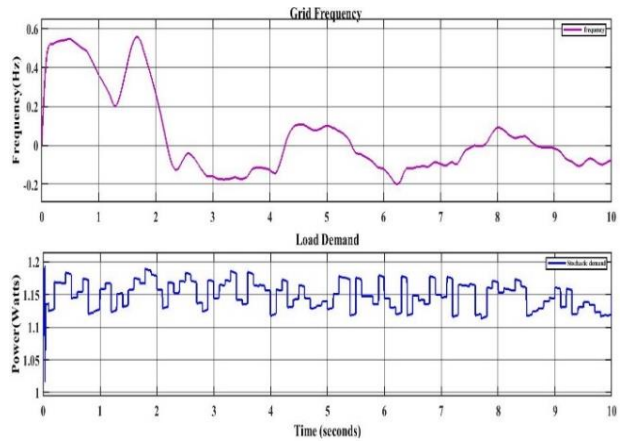


Fig. 19. Grid frequency with 100% load varying system.

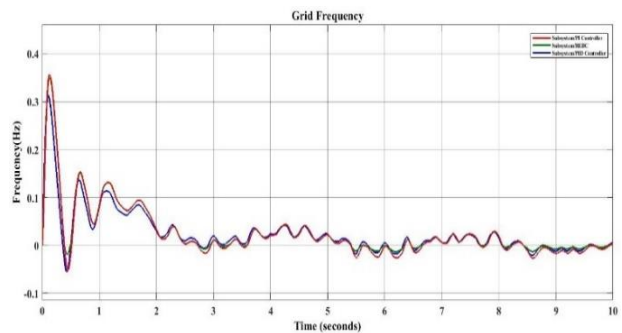


Fig. 20. Grid frequency based on different control approaches.

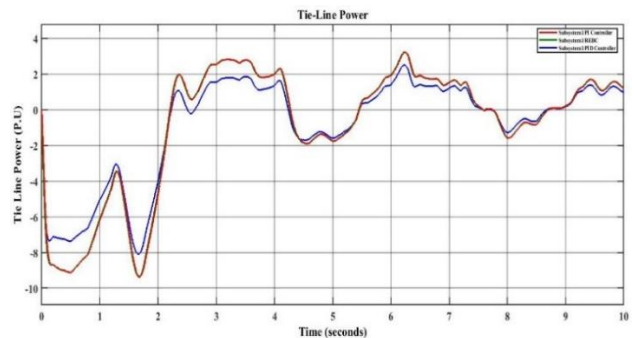


Fig. 21. Tie Line power stability analysis for 100% load system.

The system's dynamic load fluctuation will create higher frequency variation, however, the suggested REBC would provide reduced frequency variation during 100% load circumstances, as illustrated in figure 20.

The suggested multi source-single area interconnected model's tie-line power stability analysis under 100 percent load changing situations is shown in Figure 21. The PI, PID, and REBC controllers were shown to be the most effective when compared to the other controllers. Under 50 percent load varying situations, the REBC performs well.

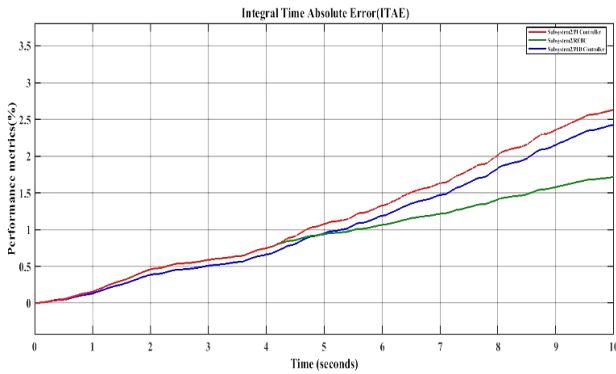


Fig. 22. ITAE using different control technique

Figure 22 illustrates the Integral Time Absolute Error (ITAE) employing various control strategies in a system with a 100% load variation. REBC calculates a 4.0 percent error ratio based on this ITAE analysis.

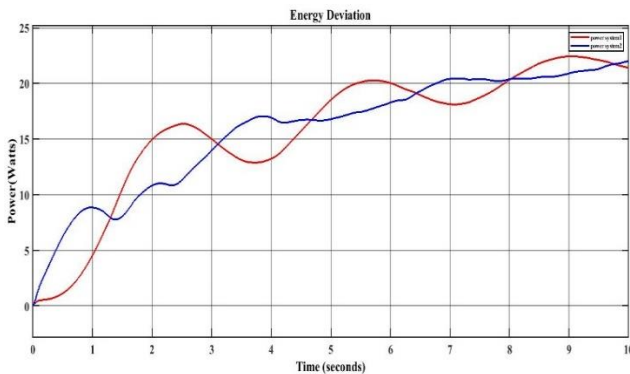


Fig. 23. Energy deviation using different control techniques

The maximum amount of load change for the MSSA Interconnected Power System is shown in figure 23. Dynamic conditions are examined for 100 percent load; the suggested REBC controller performs better in power system 1 (solar) and power system 2 (wind) energy sources.

The suggested Area-based Performance Analysis of the proposed model is shown in Table 1. The suggested model gives an effective outcome based on the aforementioned parameters, settling time (sec), Peak Overshoot (%), and Steady-state error (%).

The comparative examination of the several source locations of the linked system is shown in Figure 24. The performance of the power system-1, power system-2, and the tie-line system is evaluated using several criteria such as Settling Time (sec), Peak Overshoot (%), and Steady-state Error (%).

Table 1. Performance analysis of the proposed model based on different aspects.

Variations	Parameters	PI controller	PID Controller	REBC controller
Power system-1 (Thermal and Solar)	Settling Time(sec)	0.59	0.47	0.37
	Peak Overshoot (%)	0.089	0.069	0.039
	Steady-state error (%)	0.6.9	0.58	0.39
Power system-2 (Hydro and Wind)	Settling Time(sec)	0.55	0.39	0.34
	Peak Overshoot (%)	0.071	0.064	0.033
	Steady-state error (%)	0.64	0.48	0.35
Tie Line	Settling Time(sec)	0.52	0.40	0.34
	Peak Overshoot (%)	0.070	0.058	0.032
	Steady-state error (%)	0.60	0.45	0.31

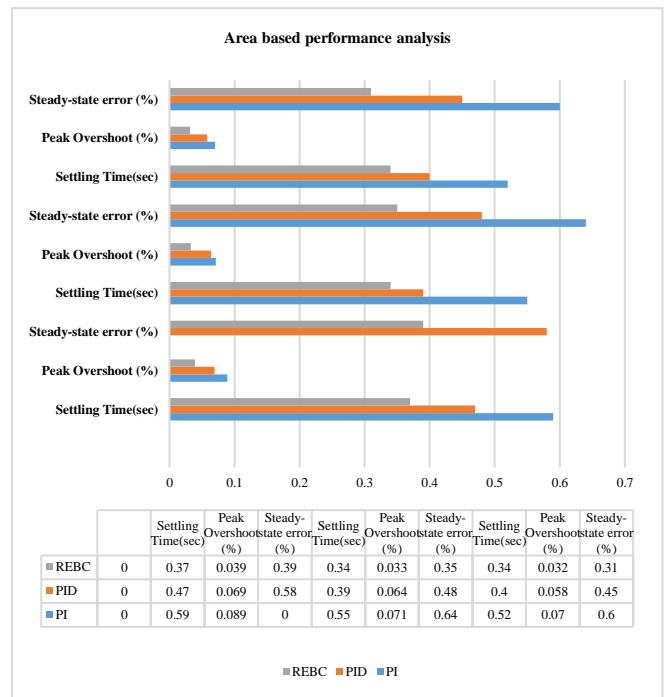


Fig. 24. Comparison analysis based on the different areas of the interconnected system.

The performance evaluation of the suggested model with and without the REBC controller is shown in Table 2. Based on the examination of several characteristics such as Peak Time (sec), Peak Overshoot (%), and Steady-state error (%) the suggested REBC controller outperforms with and without controller model.

Table 2. Performance analysis of the proposed model with and without the controller.

Variations	Parameters	Without REBC Controller	With REBC Controller	% Improvement
Power system-1 (Thermal and Solar)	Peak Time(sec)	0.70	0.35	30.21
	Peak Overshoot (%)	0.075	0.040	37.67
	settling time (sec)	0.70	0.44	27.36
Power system-2 (Hydro and Wind)	Peak Time(sec)	0.70	0.36	34.65
	Peak Overshoot (%)	0.075	0.035	35.79
	Steady-state error (%)	0.65	0.38	29.64
Tie Line	Peak Time(sec)	0.70	0.35	30.16
	Peak Overshoot (%)	0.073	0.036	36.64
	settling time (sec)	0.63	0.34	30.33

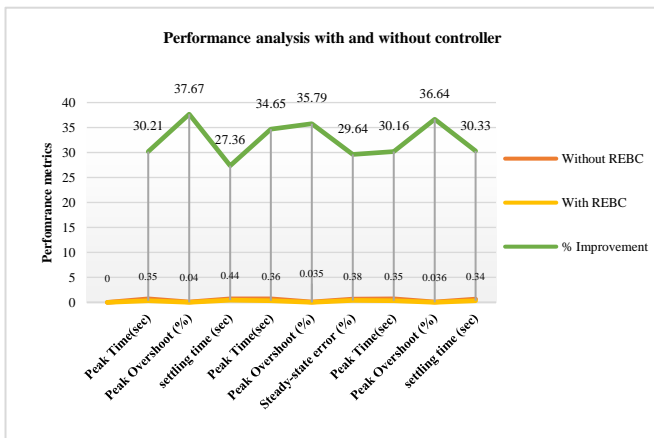


Fig. 25. Comparative analysis based on with and without a controller.

Figure 25 shows a comparison of the connected system's different source areas with and without the REBC controller. The proposed REBC controller outperforms both the controller model and the model without it, according to the findings of the previous work.

The damping measures, such as the value of the ITAE index, the maximum peak value (M_p), peak time (T_p), and settling time (T_s) Parameters are analysed with system oscillation mode (20%, 50%, and 100%), and damping Ratio (ζ) relative to the proposed controller are determined in table 3.

Table.4 represents the proposed MSSA interconnected system's performance analysis function using different control techniques like PI, PID, and the proposed REBC

control systems; based on the analysis, the proposed REBC techniques produce a better result.

Table 3. System damping characteristics with the optimized controllers.

System Oscillatory modes	ζ	F(Hz)	ITAE	M_p	T_p	T_s
20% oscillatory mode	0.824	49.54	1.46	0.0441	3.754	0.3
50% oscillatory mode	0.604	49.61	2.0	0.0393	2.432	0.44
100% oscillatory mode	0.489	49.38	4.0	0.0453	3.31	0.52

Table 4. MSSA interconnected system Performance analysis function of proposed system using REBC and existing systems.

Parameters	PI	PID	REBC
Steady-state error (%)	1.8	1.2	0.6
Settling time (sec)	0.46	0.38	0.29
Overshoot (%)	0.079	0.045	0.024
Integral Time Absolute Error (ITAE) (%)	0.0621	0.0458	0.026
Efficiency (%)	87.5	89.9	92.5

PERFORMANCE COMPARISON OF VARIOUS PARAMETER SYSTEM

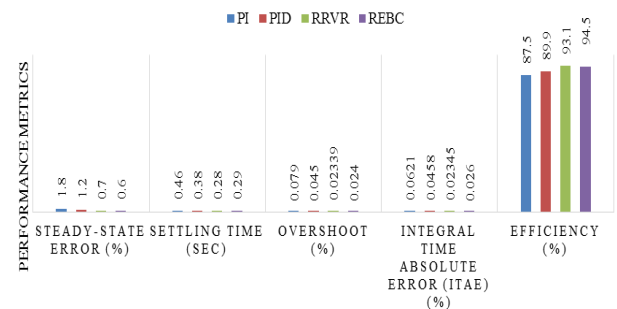


Fig. 26. Performance analysis of the MSSA interconnected system.

Figure 26 illustrates a comparison of the MSSA interconnected power system using different characteristics such as steady-state error (%), settling time (sec), overshoot (%), and Integral Time Absolute Error (ITAE). The suggested REBC may offer reliable results when compared to other current controllers like Proportional Integral (PI), Proportional Integral and Derivative (PID) and Resilience Random Variance Reduction Technique (RRVR), according to the effective comparison analysis.

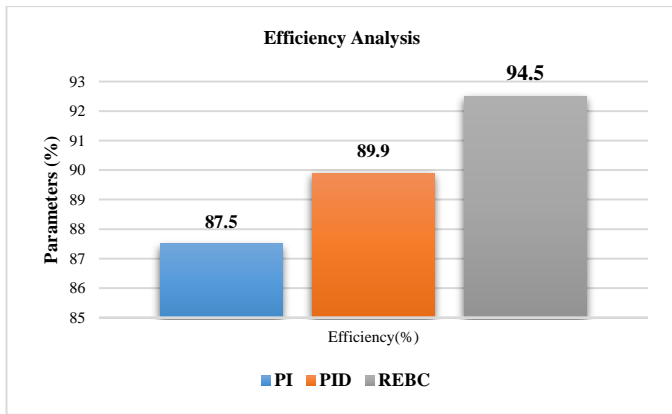


Fig. 27. Efficiency analysis.

Figure 27 shows the efficiency analysis for the proposed model. Based on this analysis, the REBC system produces 94.5 %, which is better than the existing techniques.

4. EVALUATION OF THE PROPOSED AND EXISTING CONTROL STRATEGY

The proposed solar fed DVR operation and proposed Resilience Random Variance Reduction Technique (RRVR) and Revolutionary Energy Balance Control (REBC) controllers based architecture has been developed, and its unique operation is evaluated in MATLAB Simulink.

Table 5. Comparison analysis based on the steady-state condition.

Method	Steady-State Error (%)
PI	1.8
PID	1.2
RRVR	0.7
REBC	0.6

Table 5 demonstrates the comparative analysis of the proposed Multi Area-Multi Source (MAMS) power generation model based on the Steady-State Error (%). From the comparison, it is confirmed that the proposed Revolutionary Energy Balance Control (REBC) controller produces better results than the conventional controllers.

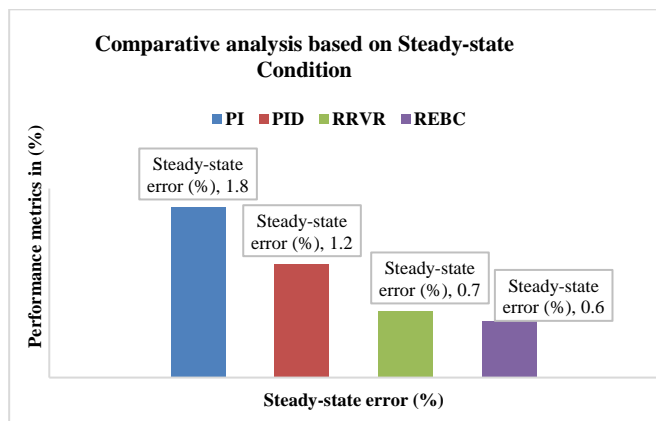


Fig. 28. Comparative analysis based on the steady-state condition.

Figure 28 represents the comparative analysis based on the steady-state condition. The comparison of the above parameters confirmed that the proposed Revolutionary Energy Balance Control (REBC) controller produces an effective result of 0.6 % steady-state condition.

Table 6. Performance analysis based on-peak overshoot.

Method	Peak overshoot (%)
PI	0.079
PID	0.045
RRVR	0.02339
REBC	0.024

The performance analysis based on peak overshoot is shown in Table 6. Peak overshoot is a way for measuring the performance of different controllers by analyzing the difference between the set point and process variable of time independent of the size. These performance standards are important since the standard peak is analyzed under various load conditions. The proposed Revolutionary Energy Balance Control (REBC) controller produces an effective result based on the table above result.

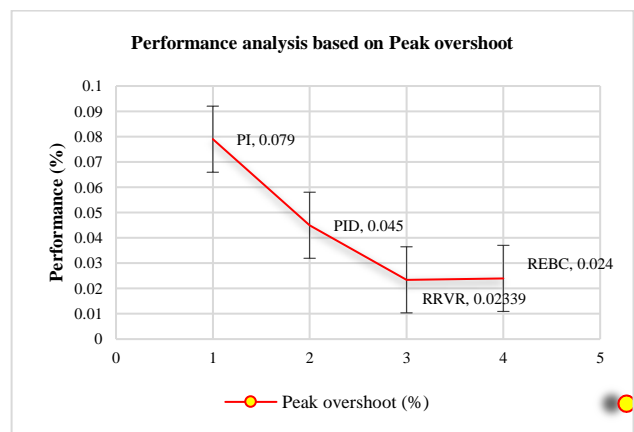


Fig. 29. Comparative analysis for peak overshoot.

Figure 29 shows the performance analysis of the proposed Multi Area-Multi Source (MAMS) power generation model. The analysis confirmed that the proposed Revolutionary Energy Balance Control (REBC) controller produces a better result based on the Peak overshoot of 0.024 (%) compared to the other existing methods.

Table 7. Integral Time Absolute Error (ITAE).

Control Techniques	ITAE (%)
PI	0.0621
PID	0.0458
RRVR	0.02345
REBC	0.026

Table 7 describes the Integral Time Absolute Error (ITAE) analysis of the proposed MSSA interconnected system's performance. For the performance analysis of the different control systems, the proposed model analyses Integral Time Absolute Error (ITAE).

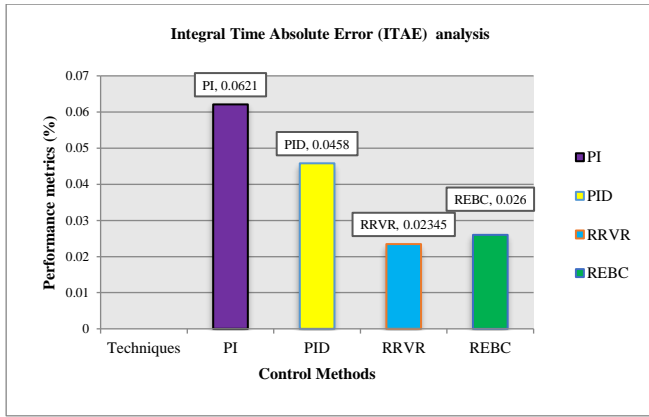


Fig. 30. Integral Time Absolute Error (ITAE).

The above figure 30 shows the Integral Time Absolute Error (ITAE) analysis of the proposed MSSA interconnected system's performance. Based on the above comparison chart, it is confirmed that the proposed REBC controller generates a 0.026 %.

Table 8. Performance analysis for settling time.

Method	Settling time (sec)
PI	0.46
PID	0.38
RRVR	0.28
REBC	0.26

From the simulation result, the Settling time performance comparison is analyzed in the above Table 8. This comparison Table shows that the REBC controller generates the Settling time ratio of 0.26 sec, which is better when compared with the other conventional controllers.

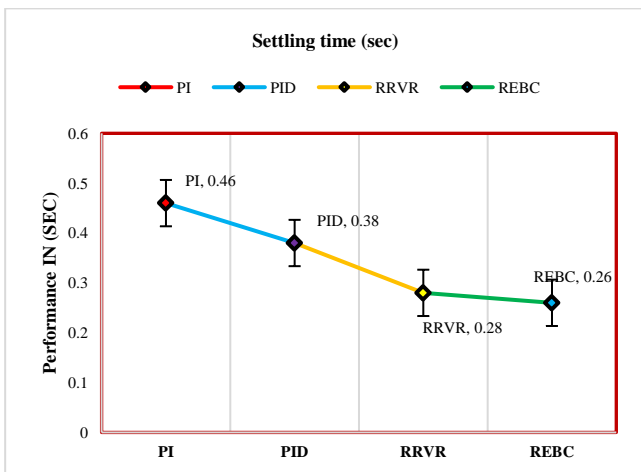


Fig. 31. Performance evaluation based on the settling time.

Figure 31 shows the Settling time performance analysis of the various controllers like PI, PID, RRVR and REBC. The proposed REBC controller will settle in the least time 0.26 sec, which is less than all the aforementioned controllers.

Table 9 shows the comparative efficiency analysis of the proposed Multi Area-Multi Source (MAMS) power generation

model. From the above comparison analysis, it is understood that the proposed REBC produces better results than the existing methods.

Table 9. Efficiency analysis.

Parameter/Method	PI	PID	RRVR	REBC
Efficiency (%)	87.5	89.9	93.1	94.5

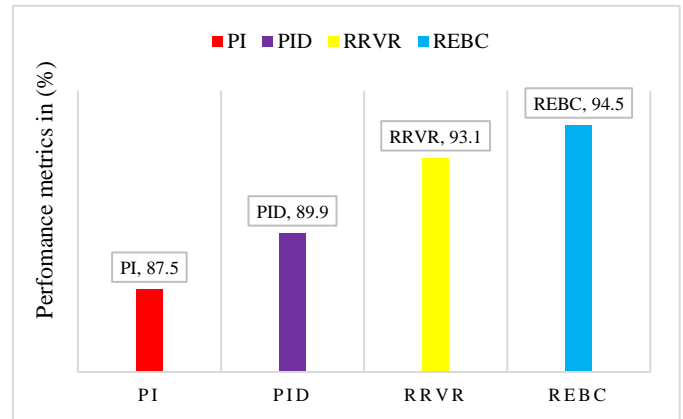


Fig. 32. Efficiency analysis.

Figure 32 shows the proposed system's efficiency analysis. From the results obtained, it is confirmed that the proposed REBC control strategy output produces better efficiency compared with the traditional methods.

Table 10. Performance analysis of the proposed models based on different aspects.

Variation	Parameter	PI controller	PID controller	RRVR controller	REBC controller
Power system-1	Settling Time(sec)	0.59	0.47	0.41	0.37
	Peak Overshoot (%)	0.089	0.069	0.048	0.039
	Steady-state error (%)	0.69	0.58	0.50	0.39
Power system-2	Settling Time(sec)	0.55	0.39	0.39	0.34
	Peak Overshoot (%)	0.071	0.064	0.045	0.033
	Steady-state error (%)	0.64	0.48	0.31	0.35
Tie Line	Settling Time(sec)	0.52	0.40	0.32	0.34
	Peak Overshoot (%)	0.070	0.058	0.046	0.032
	Steady-state error (%)	0.60	0.45	0.38	0.31

Table 10 shows the performance evaluation of the system's implemented Multi-Area Interconnected Power System (MIPS) with various controllers. Based on the parameters below, settling time (sec), Peak Overshoot (%), and steady-state error (%), the proposed REBC based model produces an effective result.

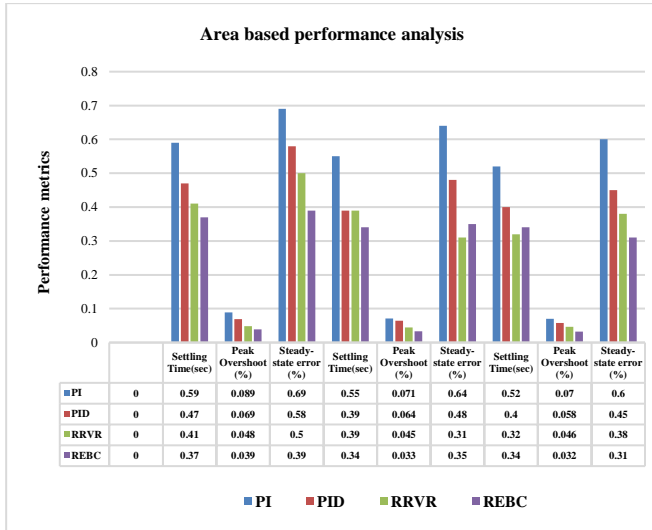


Fig. 33. Comparison analysis based on the different areas of the MIPS system.

Figure 33 shows the results of comparing the linked system's various source locations. Several criteria are used to evaluate the performance of power system-1, power system-2, and the tie-line system, including Settling Time (sec), Peak Overshoot (%), and Steady-state Error (%).

Table 11. Performance analysis of the proposed model with and without the controller.

Variation	Parameter	Without REBC Controller		With REBC controller		% Improvement of the REBC
		RRRVR	RREBC	RRRVR	RREBC	
Power system-1	Peak Time(sec)	0.76	0.70	0.38	0.35	30.21
	Peak Overshoot (%)	0.081	0.075	0.045	0.040	37.67
	settling time (sec)	0.73	0.70	0.48	0.44	27.36
Power system-2	Peak Time(sec)	0.76	0.70	0.39	0.36	34.65
	Peak Overshoot (%)	0.076	0.075	0.040	0.035	35.79
	Steady-state error (%)	0.69	0.65	0.43	0.38	29.64
Tie Line	Peak Time(sec)	0.75	0.70	0.39	0.35	30.16
	Peak Overshoot (%)	0.076	0.073	0.038	0.036	36.64
	settling time (sec)	0.65	0.63	0.39	0.34	30.33

The performance evaluation of the suggested model with and without the REBC controller is shown in Table 11. Based on the examination of several characteristics such as peak Time (sec), Peak Overshoot (%), and Steady-state error (%), the suggested REBC controller outperforms with and without the controller model.

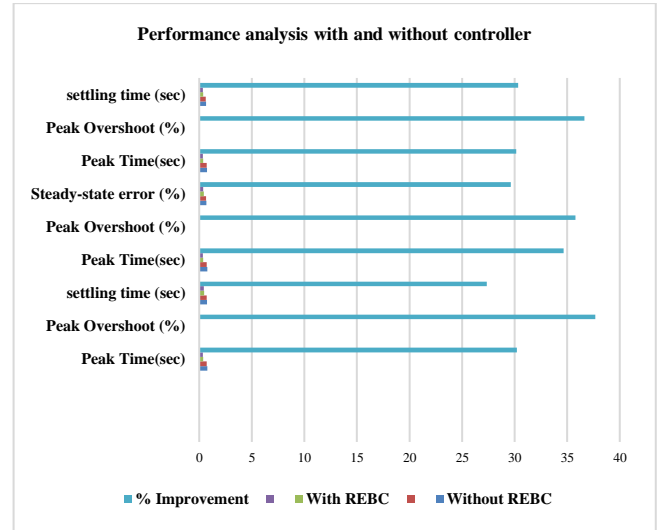


Fig. 34. Comparative analysis based on with and without a controller.

Figure 34 compares the connected system's different source areas with and without the REBC controller. The proposed REBC controller outperforms both the controller model and the model without it, according to the findings of the previous work.

Table 12. Load Variation based power quality analysis.

Input voltage (v)	Current (A)	Load (Watts)	RRVR Simulation Steady-State error (%)	REBC Simulation Steady-State error (%)
380	1.5	500	0.48	0.29
380	2.7	1000	0.59	0.33
380	4	1500	0.61	0.36
380	5.3	2000	0.7	0.4

Table 12 represents the simulation analysis of the proposed Multi Area-Multi Source (MAMS) power generation based on dynamic load conditions. Based on the variation of the load system (500-2000), the implemented RRVR and REBC controller's performances are analyzed based on the Steady-State error (%) condition. From this comparison, it is confirmed that the proposed REBC controller produces a better result.

Figure 35 determines the performance analysis of the proposed Multi Area-Multi Source (MAMS) power generation with different control approaches. From this analysis, the different load conditions, based on the steady-state performance error (%), are based on comparing REBC controllers that provide better results than the existing controllers.

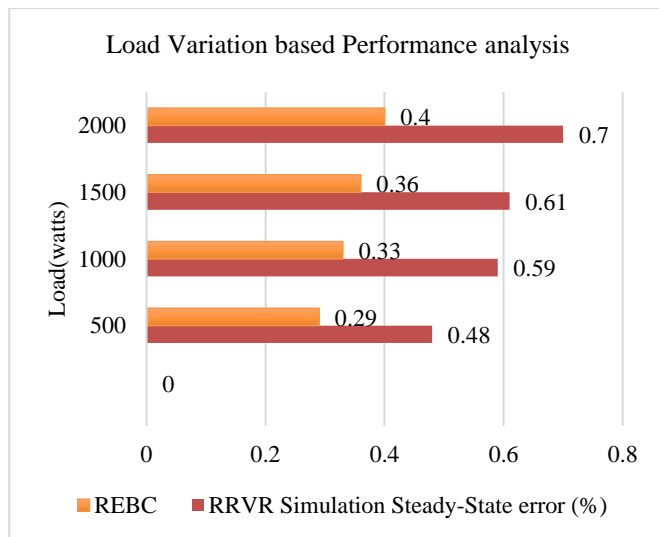


Fig. 35. Performance analysis based on load variation.

5. CONCLUSION

In this work operating frequency is a critical performance indicator for power system stability and security. During nominal power system operation, the system's frequency should be within a very limited and acceptable interval around its nominal value. AGC controllers are widely used to modulate system frequency depending on control center actions in order to create an actual power balance between generation and load. Dynamic responses have been seen in a power system using a REBC adjusted AGC controller. The optimal gains of generation-based AGC controllers are determined by the scheduled load allocated by numerous sources of power generation. The proposed Revolutionary Energy Balance Control (REBC) controller techniques are assessed and compared with existing control techniques using a number of parameters, including steady-state error (0.6%) and system efficiency (94.5 %).

REFERENCES

- Anbarasi. S and Muralidharan. S, (2016). Enhancing the Transient Performances and Stability of AVR System with BFOA Tuned PID Controller, *Control Engineering and Applied Informatics*, 18, 20-29.
- Apostolopoulou. D, Dominguez-Garcia, A and Sauer. P. W. (2016). An Assessment of the Impact of Uncertainty on Automatic Generation Control Systems, *IEEE Transactions on Power Systems*, 31, 2657-2665.
- Beyda Tasar, Hasan Güler and mehmet Ozdemir, (2015). The Investigation of Fuzzy Logic-PI Based Load Frequency Control of Keban HEPP. *Control Engineering and Applied Informatics*, 4, 71-80.
- Chen. X, Lin. J, Liu. F and Song. Y, (2019). Optimal Control of AGC Systems Considering Non-Gaussian Wind Power Uncertainty, *IEEE Transactions on Power Systems*, 34, 2730-2743.
- Daraz. A, Malik. S.A, Mokhlis. H, Haq. I.U, G. F. Laghari and N. N. Mansor, (2020). Fitness Dependent Optimizer-Based Automatic Generation Control of Multi-Source Interconnected Power System With Non-Linearities, *IEEE Access*, 8, 100989-101003.
- Daraz. A, Malik. S.A, Mokhlis. H, Haq. I.U, Zafar. F and Mansor. N.N, (2020). Improved-Fitness Dependent Optimizer Based FOI-PD Controller for Automatic Generation Control of Multi-Source Interconnected Power System in Deregulated Environment, *IEEE Access*, 8, 197757-197775.
- Dong. X. (2017). Power Flow Analysis Considering Automatic Generation Control for Multi-Area Interconnection Power Networks, *IEEE Transactions on Industry Applications*, 53, 5200-5208.
- Fakharian. A., Rahmani. R, (2016). An Optimal Controlling Approach for Voltage Regulation and Frequency Stabilization in Isolated Microgrid System, *Control Engineering and Applied Informatics*, 18, 107-114.
- Ganger. D, Zhang. J and Vittal. V. (2018). Forecast-Based Anticipatory Frequency Control in Power Systems, *IEEE Transactions on Power Systems*, 33, 1004-1012.
- Kammer. C and Karimi. A, (2019). Decentralized and Distributed Transient Control for Microgrids, *IEEE Transactions on Control Systems Technology*, 27, 311-322.
- Lackner. C, Osipov. D, Cui. H and Chow. J.H, (2020). A Privacy-Preserving Distributed Wide-Area Automatic Generation Control Scheme, *IEEE Access*, 8, 212699-212708.
- Li. J and Yu. T, (2020). Deep Reinforcement Learning Based Multi-Objective Integrated Automatic Generation Control for Multiple Continuous Power Disturbances, *IEEE Access*, 8, 156839-156850.
- Li. Z, Zang. C, Zeng. P, Yu. H and Li. H. (2016). MAS based distributed automatic generation control for cyber-physical microgrid system, *IEEE/CAA Journal of Automatica Sinica*, 3, 78-89.
- Liu, S., Liu, P. X and Saddik, A. E. (2015). Modeling and Stability Analysis of Automatic Generation Control Over Cognitive Radio Networks in Smart Grids, *IEEE Transactions on Systems, Man, and Cybernetics: Systems*, 45, 223-234.
- Patel. R, Li. C, Meegahapola. L, McGrath. B and Yu. X, (2019). Enhancing Optimal Automatic Generation Control in a Multi-Area Power System with Diverse Energy Resources, *IEEE Transactions on Power Systems*, 34, 3465-3475.
- Pathak. N, Bhatti. T.S, Verma. A and Nasiruddin. I, (2018). AGC of Two Area Power System Based on Different Power Output Control Strategies of Thermal Power Generation, *IEEE Transactions on Power Systems*, 33, 2040-2052.
- Prakash Ayyappan. B and Kanimozhi. R. (2021). Design and Analysis of the Performance of Multi-source Interconnected Electrical Power System using Resilience Random Variance Reduction Technique, *Bulletin of the Polish Academy of Sciences Technical Sciences*, 69, 1-14.
- Prostejovsky. A.M, Marinelli. M, Rezkalla. M, Syed. M.H and Guillo-Sansano. E, (2018). Tuningless Load Frequency Control through Active Engagement of Distributed Resources, *IEEE Transactions on Power Systems*, 33, 2929-2939.

- Qiu. Y, Lin. J, Liu. F and Song. Y, (2020). Explicit MPC Based on the Galerkin Method for AGC Considering Volatile Generations, *IEEE Transactions on Power Systems*, 35, 462-473.
- Sahin. E, (2020). Design of an Optimized Fractional High Order Differential Feedback Controller for Load Frequency Control of a Multi-Area Multi-Source Power System with Nonlinearity, *IEEE Access*, 8, 12327-12342.
- Shiltz. D.J, Baros. S, Cvetković. M and Annaswamy. A.M, (2019). Integration of Automatic Generation Control and Demand Response via a Dynamic Regulation Market Mechanism, *IEEE Transactions on Control Systems Technology*, 27, 631-646.
- Simpson-Porco. J.W, (2021). On Area Control Errors, Area Injection Errors, and Textbook Automatic Generation Control, *IEEE Transactions on Power Systems*, 36, 557-560.
- Tan. C, (2020). Multi-Area Automatic Generation Control Scheme Considering Frequency Quality in Southwest China Grid: Challenges and Solutions, *IEEE Access*, 8, 199813-199828.
- Van Van Huynh, Hoang-Duy Vo, Bach Hoang Dinh, Thanh-Phuong Tran and Minh Hoang Quang Tran, (2018). A New Adaptive Second Order Sliding Mode Control Design for Complex Interconnected Systems, *Control Engineering and Applied Informatics*, 20, 3-14.
- Vijayakumar. K and Manigandan. T, (2016), Nonlinear PID Controller Parameter Optimization using Enhanced Genetic Algorithm for Nonlinear Control System, *Control Engineering and Applied Informatics*, 18, 3-10.
- Wang. H, Lei. Z, Zhang. X, Peng. J and Jiang. H, (2019). Multiobjective Reinforcement Learning-Based Intelligent Approach for Optimization of Activation Rules in Automatic Generation Control, *IEEE Access*, 7, 17480-17492.
- Xi.L, (2020). A Virtual Generation Ecosystem Control Strategy for Automatic Generation Control of Interconnected Microgrids, *IEEE Access*, 8, 94165-94175.
- Xu. Y, Li. F, Jin. Z and Hassani Variani. M, (2016). Dynamic Gain-Tuning Control (DGTC) Approach for AGC With Effects of Wind Power, *IEEE Transactions on Power Systems*, 31, 3339-3348.
- Zhang. J and Domínguez-García. A.D, (2018). On the Impact of Measurement Errors on Power System Automatic Generation Control, *IEEE Transactions on Smart Grid*, 9, 1859-1868.
- Zhang. X. S, Yu. T, Pan. Z. N, Yang. B and Bao. T. (2018). Lifelong Learning for Complementary Generation Control of Interconnected Power Grids with High-Penetration Renewables and EVs, *IEEE Transactions on Power Systems*, 33, 4097-4110.